ANALYSIS OF DENTED PIPELINES CONSIDERING CONSTRAINED AND UNCONSTRAINED DENT CONFIGURATIONS

Christopher R. Alexander
Stress Engineering Services, Inc.
Houston, Texas

ABSTRACT

The American Petroleum Institute sponsored a research program starting in 1996 to determine the effects of smooth dents and rock dents on the integrity of liquid pipelines. Forty-four different dent configurations were used in the course of testing. While the primary thrust of the work was experimental, analytical efforts were made to address dent mechanics using finite element methods. A test matrix using seventy-two test cases was developed to assess the effects of pipe D/t, dent profile and depth, level of constraint and different pressure cycles on the fatigue life of dented pipelines. Results were examined in terms of stress changes resulting from denting, pressurization, and the associated residual stress states.

The shell model finite element results permitted the development of stress concentration factors for use in calculating fatigue lives for the respective dent configurations. Favorable results were obtained in comparing the calculated values to the experimentally-determined fatigue lives.

The project had two primary contributions to the study of dent mechanics. First, the program illustrates how finite element methods can be used to compare the effects of different size dents involving different pipe geometries. Secondly, as in-line inspection technology evolves, there will be an increased need to assess dents based upon their size and shape. The analytical results and methods of this research program can serve as the foundational basis for this type of correlation.

INTRODUCTION

While a considerable amount of experimental research on dents and mechanical damage have been conducted (Fowler et al., 1995 and Kiefner et al., 1996), use of finite element models permits quantitative assessment of dents not specifically addressed in experimental research programs. This benefit is derived by studying the dents in terms of stress changes resulting from denting, pressurization and the associated residual stress-states.

Information is presented herein relating to the following topics of discussion,

- Finite Element Methodology (brief background on finite element modeling and its application)
- Analysis Test Matrix (basis for selected pipe and dent geometries)
- Analytical Results (results for each defect combination)
- Verification and Application of Analytical Results (correlation with experimental work and usage of finite element data in assessing defect severity)
- Discussion of Results (meaning, comparison, and implications)

FINITE ELEMENT METHODOLOGY

A detailed description of the principles associated with finite element analyses is outside the scope of this paper; however, the basic components and variables involved will be discussed. Certain parameters are required as input into the finite element model,

- Boundary conditions
- Model configurations (element types, loading sequence, and contact issues)
- Material model.

Boundary Conditions

The boundary conditions are selected based upon the specific model geometry. To minimize computational time in the analysis phase, a quarter-symmetry model was used. Shown in **Figure 1** is a mesh for the 12-in nominal diameter pipe models used in the analysis. As illustrated in this figure, a dense mesh is applied locally to the dented region of the pipe. Also shown are the associated boundary conditions for each of the exposed edges of the model. The model was constructed using the PATRAN modeling package (version 3.1) and analyzed using the ABAQUS (version 5.4) general-purpose finite element program.

Model Configuration

The complex geometry created by the dents under review prevented a plane-strain formulation (two-dimensional), hence a three-dimensional shell model was used. Solid continuum elements were not required because of the high radius to wall thickness ratio (on the order of 34). Shell elements are permitted whenever this ratio is 10 or higher. The ABAQUS *S4R5* first-order quadrilateral shell elements were employed. These elements permit calculation of membrane strain in addition to the associated bending strains which vary as functions of thickness in the direction of the element normal vector. Transverse shear strains were also

calculated, although for piping models these are rather inconsequential in comparison to the hoop and axial strains resulting from pressure and denting. In constructing the models, all elements were oriented so that their normals projected radially outward from the axis of the pipe. In the application of pressure, a corresponding pressure was applied to the inside face of each element (due to the orientation of the element normals this corresponds to the inside of the pipe).

Because of the large strains and displacements associated with denting a pipe, the analysis accounted for stress stiffening and employed the formulation for large displacements and rotations. As one would expect, the model was highly nonlinear because of the large displacements and rotations, the nonlinear aspects of the material data, and the use of contact elements at the interface between the pipe and testing apparatus. An elastic modulus of 29 X 10^6 psi and a Poission's ratio of 0.3 were used.

The dimensions for the pipe models were 12.75-in outer diameters, wall thicknesses of 0.188-in and 0.375-in, and the lengths of the pipes were 30 inches total (approximately 2.5 diameters from the center of the dent). The longitudinal length of the pipe was selected in order to minimize any interaction between the dent area and the end of the pipe.

The basic components of the model from a construction standpoint were:

- Pipe material
- Indenter
- Saddle.

The geometry for the indenters was equivalent to those used in the experimental work (Alexander and Kiefner, 1997). Refer to the information provided in **Table 1** for dimensions on the indenters. As illustrated in **Figure 1**, the saddle supports the bottom portion of the pipe and is similar to the saddle arrangement that exists with the experimental dent set-up. The radius of curvature for the saddle was larger than the pipe radius to prevent any over-constraining the bottom of the pipe.

Contact elements were generated in all areas where contact was expected. The two areas of contact in the pipe were the dent regions between the pipe and indenter, and at the bottom of the pipe where contact with the saddle is made. As implied by its name, the contact element is used where two or more bodies come in contact. A load transfer occurs and the bodies deform based on the relative compliance of the members involved. For our application, the relative stiffness of the indenter and saddle are much greater than pipe. This means that the pipe deformed locally in relation to these contact surfaces that possess greater stiffnesses. When the indenter displacement was removed, the pipe body maintained a shape based upon the level of indentation and plasticity-level induced in the pipe. This stress configuration in the pipe is known as the residual stress state and performs a critical role in determining the alternating stresses induced in the process of cycling with internal pressure.

Both smooth and rock dents were studied in the analysis phase of this research program. The smooth dents were allowed to reround after being installed in the pipe; however, the rock dents were not permitted to reround. The latter indention remains constant during the course of pressure cycling. The terms used to describe these two dent configurations are *unconstrained* and *constrained*, respectively. In conducting the analysis, the load steps employed in denting, rebounding, and pressurizing were identical to the steps used in the experimental work. The four basic load steps for the unconstrained smooth dents were as follows:

- Indent to a depth specified as a percentage of pipe diameter
- Remove indenter and allow elastic rebound of the pipe
- Apply pressure inside the pipe
- Remove internal pressure (determination of final residual dent depth).

The three basic load steps for the constrained rock dents are as follows:

- Indent to a depth specified as a percentage of pipe diameter
- Apply pressure inside the pipe
- Remove internal pressure (determination of final residual dent depth).

Material Model

In order to accurately model the behavior of the piping material in response to denting, elastic rebound, and response to cyclic pressurization, a material model incorporating plasticity was used with an assumption of isotropic hardening. Values for the true stress/true strain input were based upon conversion of lab test data for X52 grade material.

The following sections present information relating to the matrix selected for analysis, correlation with experimental data, and usage of analytical results in predicting fatigue life.

Analysis Test Matrix

Because the experimental efforts were started prior to the finite element work, an analysis matrix was developed based upon the insights gained in the course of testing. The selection of the 12-in nominal pipe diameter was for purposes of comparison with the experimental test samples. Additional variables were also selected based upon interests not necessarily addressed in the experimental work. **Table 1** provides a complete listing of these variables and description of the indenters.

The analysis matrix provided for a total of 72 test cases. While only one pipe diameter was considered, the effects of diameter to wall thickness were addressed in considering D/t values of 34 and 68.

While typical fatigue data would lead one to believe that increased mean stress has a detrimental effect on fatigue life, experimental work illustrated the benefits associated with cycling dented pipes at upper range of the MOP. The benefit resides primarily in the removal of the associated indentations which then lowers the alternating stresses of the dented region. In light of this information, the test matrix presented in **Table 1** shows 3 cyclic pressure ranges based upon percentages of MOP (where MOP corresponds to 72% SMYS). The phenomenon has been well established by previous experimental research programs (Fowler et al., 1995 and Alexander and Kiefner, 1997).

ANALYTICAL RESULTS

Considering that 72 dent combinations were analyzed, the ability to organize the results in a meaningful manner is important for developing logical discussions and conclusions. For the reader presentation of the results is broken into six specific categories,

- Method of extracting stresses from the finite element models
- Conversion of biaxial FEA stresses to principal stresses
- Failure theory selection

- Development of non-dimensional stress concentration factors (SCF),
- Development of SCF tables using the $\Delta\sigma/\Delta P$ values, residual dent depths, and second-order polynomial curve fits
- Calculating fatigue life employing an appropriate fatigue curve and the SCF tables.

Although a review of the specific element/nodal stresses is important for assessing the fatigue performance of any dent, a colored stress contour plot aids the analyst in understanding the general stress distribution in and around the dent. It should be remembered that the stress state at any given position in the operating cycle is not as important as the range over which the material is stressed. Hence, a graphical presentation of the finite element stresses does not provide as informative an assessment of dent severity as does an analysis of the changing numerical stress values at specific locations in the dent. The latter is presented here and discussed in detail in the sections which follow.

Extracting Stresses from the Finite Element Models

As stated previously, the shell elements provided a biaxial stress state. This means that output is provided in the form of hoop, axial, and in-plane shear stresses. These stresses are known as **component** stresses. ABAQUS provides these stresses for each element including values at the inside, middle, and outside wall positions. During the analysis, stresses for the dented area of the pipe were extracted. For the unconstrained configuration, stresses were obtained at indentation, rebound, pressurization, and pressure-removal. Likewise, for the constrained case stresses were obtained at indentation, pressurization, and pressure-removal.

The primary stresses of interest are those that occur at the pressurized and unpressurized states. It is between these two levels of loading that the alternating stress occurs. The alternating stress between these two states is defined for the three component stresses (axial, hoop, and shear) as follows,

(Hoop) $S11_{alt} = S11_{pressure} - S11_{no\ pressure}$
(Axial) $S22_{alt} = S22_{pressure} - S22_{no\ pressure}$
(Shear) $S12_{alt} = S12_{pressure} - S12_{no\ pressure}$

This procedure was used for all elements in the dented region on the inside, middle, and outside sections of the pipe. Once this was completed for all of the elements of interest, the principal stresses were determined.

Conversion of Biaxial FEA Stresses to Principal Stresses

The principal stresses are the stress inputs required by most failure theories. Discussion of the selected failure theory will follow; however, this section of the paper discusses the method used to convert the biaxial stress state to a shear-free principal orientation. The principal stresses are determined by calculating the eigenvalues, λ, for the following determinant,

$$\begin{vmatrix} S11_{alt}-\lambda & S12_{alt} \\ S12_{alt} & S22_{alt}-\lambda \end{vmatrix} = 0$$

where $S11_{alt}$, $S22_{alt}$, and $S12_{alt}$ are the alternating hoop, axial, and in-plane shear stresses, respectively. The previous determinant yields the following characteristic equation,

$$\lambda^2 - (S11_{alt} + S22_{alt})\lambda + (S11_{alt} \cdot S22_{alt} - S12_{alt}^2) = 0$$

The solution for the characteristic equation is computed using the quadratic equation,

$$\lambda_{1,2} = \frac{(S11_{alt} + S22_{alt}) +/- \sqrt{(S11_{alt} + S22_{alt})^2 - 4(S11_{alt} \cdot S22_{alt} - S12_{alt}^2)}}{2}$$

The alternating component stress ranges ($S11_{alt}$, $S22_{alt}$, and $S12_{alt}$) were computed by subtracting the component stresses at the maximum pressure level from the component stresses at the minimum pressure level for each respective dent and pressure range combination. These stress ranges were then used as input for the above equations. Using this methodology, two principal stresses were computed for each element in the dented region at three wall thickness positions. These principal stresses served as the input for the failure theory.

Failure Theory Selection

There are several failure theories that could be used in the analysis of the alternating stresses for the dented pipe. The two most commonly used theories for ductile materials are,

- Maximum Shear Stress Theory
- Maximum Distortion Energy Theory (Von Mises).

While either method could be used in this study, the Maximum Shear Stress Theory is selected because of both its conservative nature and its use in the ASME Boiler & Pressure Vessel Code, Section VIII, Division 2 (Code). The methods presented in this report are basic derivations of the practices recommended by the Code for assessing fatigue performance of pressure vessels under internal pressure loading.

As the name implies, the Maximum Shear Stress Theory assumes that the onset of static failure occurs when the maximum shear stress reaches the shear yield strength of the material ($S_{yield}/2$). A review of Mohr's Circle is in order for quantifying the maximum shear stress using the computed principal stresses. **Figure 2** shows Mohr's Circle and the orientation of the stresses on a unit cube of the pipe.

As can be seen from the figure, the two largest principal stresses are those calculated from the biaxial stress-state; however, the smallest of the principal stress, σ_3, is created by the compressive load imparted on the element by the internal/external pressure differential.

The diameter of Mohr's Circle is the largest algebraic difference between the minimum and maximum principal stresses ($\sigma_1 - \sigma_3$) and is equal to two times the maximum shear stress ($2\tau_{max} = \sigma_1 - \sigma_3$). This quantity is referred to as the *stress intensity*. While the maximum shear stress is of some interest in this problem, the greater concern is the range of alternating stress intensity imparted to the local pipe body during the process of pressure cycling.

The stress intensity ranges ($\sigma_1 - \sigma_3$) for each of the elements were computed using the methods outlined above. From each defect combination (dent type and depth, pipe geometry, pressure level, and type of constraint), a maximum stress range was determined for all elements in the dented region. Hence, 72 cases produced 72 stress ranges. The assumption is that failure in the dent will be induced based upon the fatigue behavior of the element having the largest alternating stress range.

Development of Stress Concentration Factors

In order to permit application of the finite element results to a variety of pressure levels, a non-dimensional stress concentration factor (SCF), $\Delta\sigma/\Delta P$, was developed. This SCF was defined as the ratio of the stress intensity range to the range of applied pressure. Using this procedure, 72 unique stress concentration factors were developed.

Previous and ongoing research indicates that the mean pressure and corresponding pressure range must be considered in addition to the residual dent depth. The basis for this approach is that the increased pressure decreases the depth of the dent that remains in the pipe. The smaller dent depth then results in lowering the alternating stress levels in the dent. As the dent rerounds with increased pressure, the alternating stress level also decreases. Failure to account for this decrease in stress will result in calculating premature failures for the dent depth actually involved in pressure cycling.

Development of SCF Tables

One of the primary objectives of this research program is to provide pipeline operators with a method for predicting the number of cycles to failure for a given dent depth or defect type. The experimental results may be applied to certain defect combinations, assuming they have similar geometries and load histories as those tested. However, the benefit of having analytical results resides in the capacity to calculate fatigue lives for a variety of dent depths and pressure levels. Validation with experimental findings adds greater confidence in applying these analytical results.

Provided in **Tables 2** through **5** are the SCF tables calculated using the FEA results. Each of the four tables considers the following variables,

- Residual dent depth
- Stress concentration factor
- Alternating pressure level.

The tabulated values for each of the dent depths (e.g., 1%, 2%, . . .) were computed using a polynomial curve fit of the FEA data. For example, at the lower pressure level, the unconstrained dome dent with a pipe D/t ratio of 68 had SCF * values of 120.7, 188.9, and 231.0 for residual dent depths of 2.8, 6.4, and 9.0, respectively. These values were used in developing the following second-order polynomial,

$$\frac{\Delta\sigma}{\Delta P} = -0.5346\left(\frac{d}{D}\right)^2 + 24.006\left(\frac{d}{D}\right) + 57.675$$

where $\Delta\sigma/\Delta P$ represents the stress concentration factor. This procedure was done for all 72 dent cases and produced a total of 24 curves (each curve has 3 dent depths). Using these curves, the SCF values in **Tables 2** through **5** were determined for integer dent depths. As noted in several of the tables, some curve fits produced non-linearities which prohibited their use over the entire range of the tabulated dent depth levels. Based upon experimental data, the residual dent depths for the 12-inch pipe (D/t of 68) never exceeded 6% of the pipe's diameter when an internal pressure of 72% SMYS was applied, even with an initial indentation of 18%. For this reason, those SCF values not listed due to excessive non-linearities for the respective curve fits that were outside the range of practical application.

As a function of increasing residual dent depth, the stress concentration factors associated with unconstrained dents change less at high operating pressures than at low operating pressures. The reason for this is greater permanent rerounding of the dent that occurs at high pressures compared to low pressures. For example, consider results as presented below,

- 1% dome dent, D/t = 68, lower pressure range SCF=81.1
- 9% dome dent, D/t = 68, lower pressure range SCF=230.4 (289% increase from 1% dent)
- 1% dome dent, D/t = 68, upper pressure range SCF=70.7
- 9% dome dent, D/t = 68, upper pressure range SCF=143.3 (203% increase from 1% dent).

This trend is not limited to pipes with the above pipe geometry, constraint type, or dent type. The constrained dents also illustrate a similar pattern.

While two D/t ratios were considered in this research, an important question not addressed relates to the correlation between the dent diameter and the pipe diameter. In other words, the ratio of dent depth to pipe diameter is important, and much like the dent depth to pipe diameter (d/D). It should be used in quantifying defect severity. This issue is one to be dealt with in future studies.

Calculating Fatigue Life with Fatigue Curves and SCF Tables

Once the stress concentration factors and tables were developed, calculation of fatigue lives for the respective defect combinations were possible. This process was also used for validating the analytical efforts (see *Verification and Application of Analytical Results*). While numerous fatigue curves could be used, the one selected was from the ASME Boiler & Pressure Vessel Code, Section VIII, Division 2, Appendix 5 (Figure 5-110.1). This curve is for carbon steels with yield strengths less than 80 ksi. While this curve is design-oriented, it is conservative by a factor of

* By this definition the SCF for a pipe with D/t = 68 with no dent is 34. This because $\Delta S = \Delta PD/2t$ by the Barlow formula. Thus, the relative effect of any given value of SCF calculated for a pipe with D/t = 68 by the finite element analysis can be visualized by dividing the SCF by 34. For the highest value shown in **Table 2**, (244.3 for a 10 percent residual dent) the relative effect is 244.3/34 or more than a factor of 7. Even for small residual dents, however, one can see that the relative SCF can be expected to result in cyclic stress ranges 2 to 3 times as large the Barlow stress range.

two with respect to stress and twenty with respect to cycle number. The curve is described by the following equation,

$$N = \exp\left(43.944 - 2.971 \cdot \ln\left(\frac{\Delta\sigma}{2}\right)\right)$$

where $\Delta\sigma$ is computed by multiplying the SCF by the applied pressure range, ΔP.

Consider a dented pipe with the following characteristics:

Residual Dent Depth:	3 percent of pipe diameter
Pipe D/t:	68
Pressure Level	550 - 1100 psig (upper range of 50% MOP)
Dent Type:	Unconstrained Dome Dent.

For calculating the expected fatigue life for such a defect, consult **Table 2** and extract the appropriate SCF which is ***101.4*** for this problem. Using this SCF and ΔP equal to 550 psig, the fatigue life is computed to be,

$$N = \exp\left(43.944 - 2.971 \cdot \ln\left(\frac{101.4 \cdot 550}{2}\right)\right) = 754{,}120 \ cycles$$

For the same problem, consider the pressure range to be 1,100 psig (100% MOP). The SCF is found to be ***107.1*** and ΔP is equal to 1,100 psig. The fatigue life is computed to be,

$$N = \exp\left(43.944 - 2.971 \cdot \ln\left(\frac{107.1 \cdot 1100}{2}\right)\right) = 81{,}755 \ cycles$$

This set of calculations shows the significant impact that the applied pressure range has on the fatigue life, even though there is only a 5.6 percent difference in the respective stress concentration factors.

VERIFICATION OF ANALYTICAL RESULTS

The importance of validating the analytical results cannot be over-emphasized. While not all of the analytical results may be validated, there are several critical variables considered,

- Fatigue life prediction
- Load deflection curve
- Analytical versus experimental rerounding characteristics
- Experimental failure patterns.

Fatigue Life Prediction

Results for two of the experimental samples are compared to the calculated fatigue lives using the FEA-defined stress concentration factors, the modified ASME curve, and Miner's Rule. For our purposes, Miner's Rule is defined by the following equation,

$$1 = \frac{n_{50}}{N_{50}} + \frac{n_{100}}{N_{100}}$$

where:

n_{50} = number of cycles with ΔP = 50% MOP
N_{50} = maximum number of cycles with ΔP = 50% MOP (determined experimentally or analytically)
n_{100} = number of cycles with ΔP = 100% MOP
N_{100} = maximum number of cycles with ΔP = 100% MOP (determined experimentally or analytically).

As indicated in the above equation, Miner's Rule states that the useable life for a member is completed when either one or the summation of both terms equals unity. The right-hand side of the equation may be expanded to account for additional pressure ranges (e.g., n_{75}/N_{75}).

Table 6 provides a comparison of results for the experimental and analytical fatigue lives of samples *UD6A-2* and *UD12A-3* (Alexander and Kiefner, 1997). As noted in the table, an *Experimental Equivalent Number of Cycles* is provided for two of the experimental dented fatigue samples. This number represents the total number of cycles applied to each dented sample using one equivalent pressure ratio, although two different pressure ranges were applied. This is done using a fourth order relationship between cycles to failure and applied stress cycles. The equation below was used to establish this relationship.

$$N_{equiv} = n_{50} + n_{100} \cdot \left[\frac{\Delta P_{50}}{\Delta P_{100}}\right]^{-4}$$

Consider the fatigue data for Sample *UD6A-2*,

- 28,183 cycles at 50% MOP (n_{50})
- 79,940 cycles at 100% MOP (n_{100})

Substituting the appropriate terms into the above equations yields the equivalent number of cycles for UD6A-2 with an applied stress range corresponding to 50% MOP.

$$N_{equiv} = 28{,}183 + 79{,}940 \cdot \left[\frac{550 \ psi}{1{,}100 \ psi}\right]^{-4} = 1{,}307{,}223 \ cycles$$

A similar calculation was performed for Sample UD12A-3, as provided in **Table 6**.

The tabulated results indicate that a reasonably accurate method of estimating fatigue life has been developed. The results are adequately close given the inherent variability in all fatigue testing and the uncertainties in predicting fatigue life, in addition to issues relating to modeling difficulties and assumptions.

Load Displacement Curve Validation

Another method for validating the finite element results was to compare the load displacement curves generated during the denting process. While load versus deflection was not measured for many of the first experimental samples, a significant amount of data exists for the later samples. **Figure 3** provides the load deflection curves for the following defect combinations (all performed on X52 pipe, 12.75 inch O.D. by 0.188 inch wall),

- Experimental denting, dome cap indenter, d/D = 12%
- Experimental denting, long bar indenter, d/D = 12%
- Finite element denting, dome cap indenter, d/D = 12%

- Finite element denting, long bar indenter, d/D = 12%.

While there are some differences in the data plotted for the experimental and analytical results, the final loads are very close. One obvious reason for the difference is that in the experimental denting process there is some inherent slack in the set-up vertically. The figure shows for the long bar indenter that although the experimental load is initially lower than the FEA values, both values are comparable for deflections greater than 0.75 inches. The experimental and analytical results for the dome indenter are similar throughout the duration of the denting process. Additional bases for the differences could reside in the constitutive model used, such as failure to account for phenomena such as the Bauschinger effect.

Analytical versus Experimental Rerounding Characteristics

Previous experimental and analytical efforts show that depth is one of the most effective means for characterizing the severity of a dent. Obviously, additional stress concentrators such as corrosion and gouges will contribute to the deleterious nature of the smooth dent. However, these type of anomalies are not addressed in the analytical phase of this research program.

Figure 4 shows the experimental and analytical results for the dent profile measured along the axis of the pipe. It is apparent from the data plotted, that additional experimental data could be taken for creating a more complete dent profile. The predominant observation is the significant level of rerounding that occurs with the application of pressure. The final dent depth prior to pressure cycling is the level most critical in analyzing the dent's impact on fatigue life of the pipe.

Locations of Cracks Versus High-Stress Range Locations

A final point concerns the relationship that exists between the dent geometry and the pipe dimensions. The fatigue cracks in the dome dent in this program tended to occur away from the centers of the dents as created by the denting process, in an area known as the *dent periphery*. This failure pattern is consistent with the high stress-range locations from the finite element models for the dome dents. A similar trend exists with the long bar dents, especially if the long bar is considered to be an axially-extruded dome dent.

IMPLICATIONS OF THE FINITE ELEMENT RESULTS

In this section of the paper, results from the finite element work are related to the overall API research program. First, it must be recognized that this work was a cursory evaluation to show how one might generate and use stress concentration factors based on finite element analyses to compare the effects of dents of different sizes involving different pipe geometries. It does appear that the approach is valid and useful. However, much more work would be necessary to permit the analyses to be applied extensively with a high degree of confidence. Additional comparisons with experimental results would be desirable. It is likely that further comparisons would show the need to "calibrate" the model because neither the mechanics nor the material factors could be defined adequately by the size of effort undertaken in this project.

Second, as in-line inspection technology to detect mechanical damage evolves, there will be a need to rank dent-like indications based on size and shape. An expanded and well-validated version of the SCF approach developed herein could serve as the basis for dent-ranking guidelines just as the B31G criterion now does for corrosion-caused metal loss anomalies.

REFERENCES

Alexander, C. R. and J. F. Kiefner, *Effects of Smooth and Rock Dents on Liquid Petroleum Pipelines*, API Publication 1156 (First Edition), American Petroleum Institute, Washington, D.C., November 1997.

Budynas, R. G., *Advanced Strength and Applied Stress Analysis*, McGraw-Hill, New York, 1977.

Fowler, J. R., C. R. Alexander, P.J. Kovach, and L.M. Connelly, *Cyclic Pressure Fatigue Life of Pipelines with Plain Dents, Dents with Gouges, and Dents with Welds*, Prepared by Stress Engineering Services for the Offshore and Onshore Applications Supervisory Committee of the Pipeline Research Committee, PR-201-9324, 1995.

Kiefner, J. F., C. R. Alexander, and J. R. Fowler, *Repair of Dents Containing Minor Scratches*, Proceedings from Ninth Symposium on Pipeline Research, Houston, Texas, October, 1996.

Kiefner, J. F., W. A. Bruce, and D. R. Stephens, *Pipeline Repair Manual*, Prepared for the Line Pipe Research Supervisory Committee of the Pipeline Research Committee, 1994.

Maxey, W.A., *Outside Force Defect Behavior*, NG-18 Report No. 162, A.G.A. Catalog No. L51518, 1986.

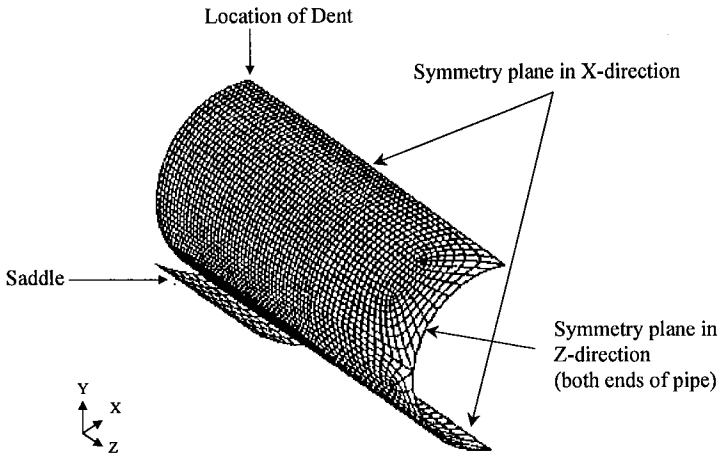

Figure 1 Quarter-symmetry Finite Element Model Mesh

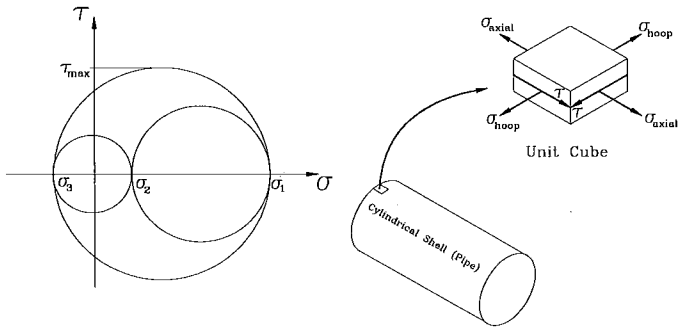

Figure 2 Mohr's Circle and Unit Cube Orientation

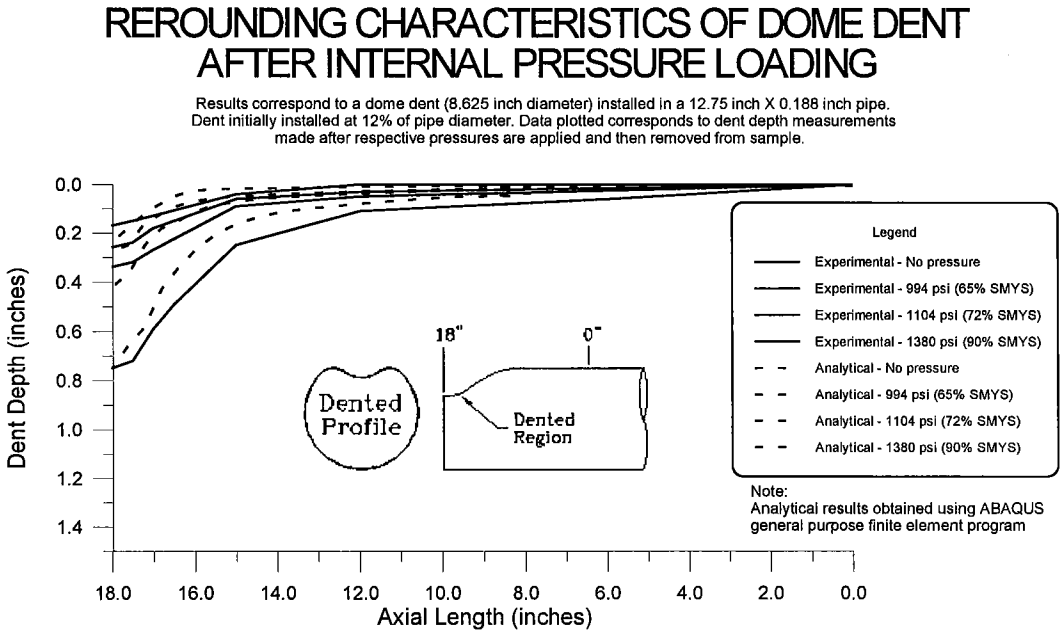

Figure 3 Comparison of Rerounding Characteristics for FEA versus Experimental Results

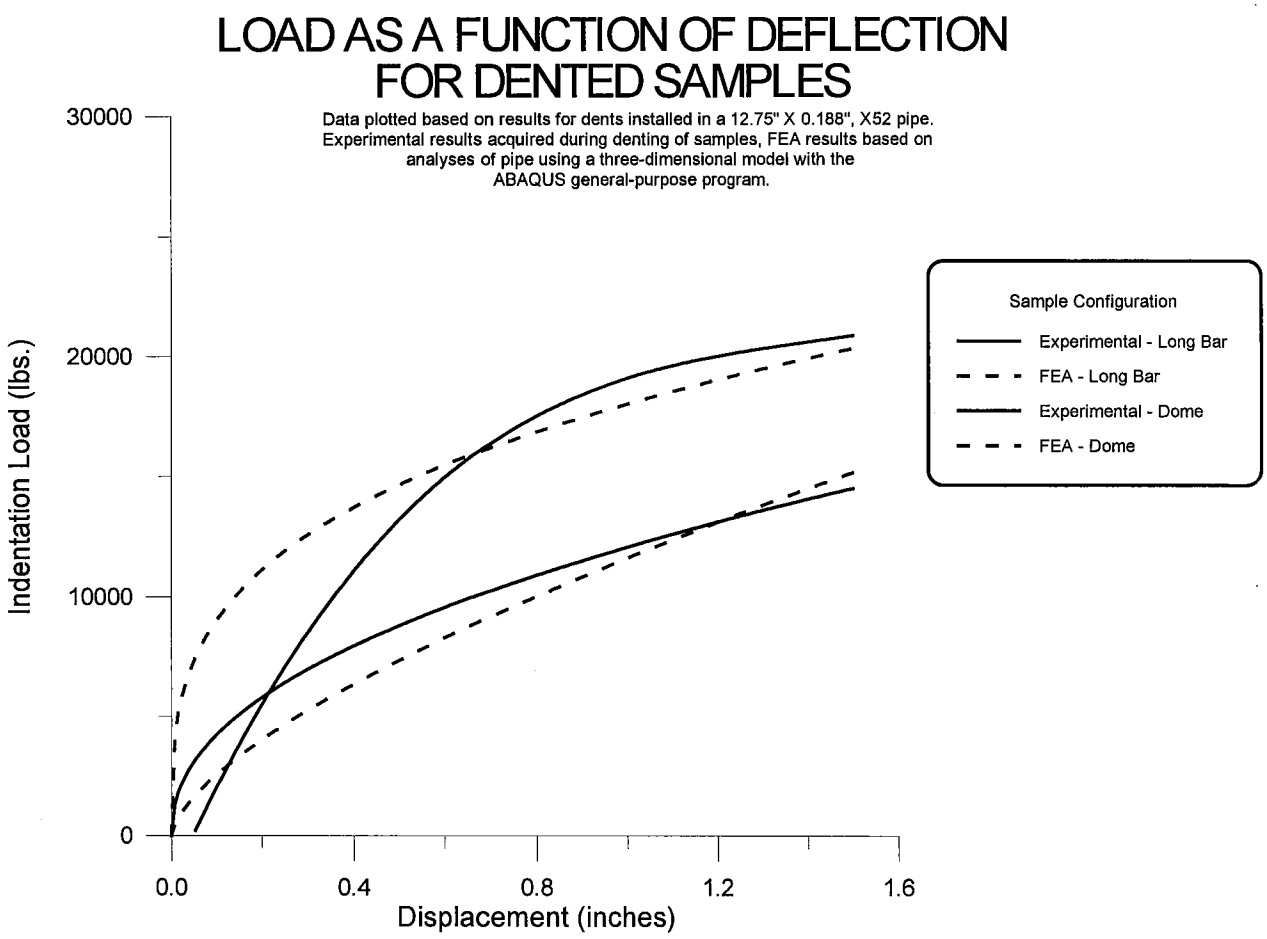

Figure 4 Load Deflection Curve for FEA versus Experimental Results

Table 1 Variables Considered in the FEA Matrix

Variable	Value
Pipe diameter to wall thickness (D/t)	34 and 68
Indenter types	Dome and Long Bar
Dent Depths (percent of pipe diameter, d/D)	6, 12, and 18%
Pressure cycles (consider effects of mean stress and upper pressure)	0 - 50% MOP 50 - 100% MOP 0 - 100% MOP
Dent boundary conditions	Constrained and Unconstrained

Notes:
1. The *dome dent* was made using a dome end cap with an outer diameter of 8.625 inches
2. The *long bar dent* was made using an indenter with a cross-sectional diameter of 4 inches and 20 inches in length.

Table 2 Stress Concentration Factors (Δσ/ΔP) for Unconstrained Dome Dents

Pipe D/t	Residual Dent Depth (percent d/D)									
	1	2	3	4	5	6	7	8	9	10
Low Range Pressure Cycle (0 - 50% MOP)										
34	***38.5***	***42.7***	47.1	51.5	56.0	60.7	65.6	70.4	75.4	80.5
68	***81.1***	103.5	128.9	145.1	164.3	182.5	199.5	215.5	230.4	244.3
High Range Pressure Cycle (50 - 100% MOP)										
34	***34.8***	38.7	42.5	46.2	49.8	53.2	56.6	59.8	62.9	65.9
68	***70.7***	87.1	101.4	113.6	123.7	131.7	***137.7***	***141.5***	***143.3***	
Full Range Pressure Cycle (0 - 100% MOP)										
34	***32.9***	38.0	42.8	47.4	51.7	55.8	59.7	63.4	66.8	70.0
68	***71.0***	90.8	107.1	119.8	128.9	134.4	***136.3***			

Notes:
1. Residual dent depths (d/D) based upon maximum analytical dent depths remaining after prescribed pressure range applied to sample for one cycle
2. Pressure ranges based upon percentage of MOP, Maximum Operating Pressure (100% MOP corresponds to 72% SMYS)
3. Tabulated SCF values based upon curve fit of FEA data using a second-order polynomial
4. Number in ***bold italics*** are extrapolated from the range of minimum and maximum residual FEA dent depths
5. Polynomial curve fitting process produced some invalid values (out of range with other values) and are indicated by cells that have been blacked out (■).

Table 3 Stress Concentration Factors (Δσ/ΔP) for Unconstrained Long Bar Dents

Pipe D/t	Residual Dent Depth (percent d/D)									
	1	2	3	4	5	6	7	8	9	10
Low Range Pressure Cycle (0 - 50% MOP)										
34	***20.9***	41.6	59.8	75.6	89.0	100.0	108.6	114.7	***118.4***	
68	***70.8***	123.3	167.5	203.3	230.9	250.1	261.0	263.6		
High Range Pressure Cycle (50 - 100% MOP)										
34	***27.0***	41.6	54.2	64.8	73.4	80.0	***84.7***	***87.4***	***88.0***	
68	63.7	86.8	105.3	119.4	***129.0***	***134.2***	***134.9***			
Full Range Pressure Cycle (0 - 100% MOP)										
34	***28.6***	44.8	58.1	68.3	75.6	79.8	***81.1***			
68	70.9	102.0	123.8	136.1	139.0					

Notes:
1. Residual dent depths (d/D) based upon maximum analytical dent depths (measured in dimple region of dent) remaining after prescribed pressure range applied to sample for one cycle
2. Pressure ranges based upon percentage of MOP, Maximum Operating Pressure (100% MOP corresponds to 72% SMYS)
3. Tabulated SCF values based upon curve fit of FEA data using a second-order polynomial
4. Number in ***bold italics*** are extrapolated from the range of minimum and maximum residual FEA dent depths
5. Polynomial curve fitting process produced some invalid values (out of range with other values) and are indicated by cells that have been blacked out (■).

Table 4 Stress Concentration Factors (Δσ/ΔP) for Constrained Dome Dents

Pipe D/t	Dent Depth (percent d/D)								
	2	4	6	8	10	12	14	16	18
Low Range Pressure Cycle (0 - 50% MOP)									
34	33.6	42.6	50.4	57.1	62.7	67.2	70.6	72.8	73.9
68	***128.5***	138.7	148.8	159.0	169.1	179.3	189.4	199.6	209.7
High Range Pressure Cycle (50 - 100% MOP)									
34	33.7	37.5	40.8	43.8	46.3	48.5	50.3	51.7	52.7
68	73.1	77.2	81.3	85.5	89.6	93.7	97.8	101.9	106.0
Full Range Pressure Cycle (0 - 100% MOP)									
34	***37.6***	40.5	43.3	45.8	48.2	50.3	52.2	53.9	55.4
68	84.4	88.2	92.1	95.9	99.7	103.6	107.4	111.2	115.1

Notes:
1. Pressure ranges based upon percentage of MOP, Maximum Operating Pressure (100% MOP corresponds to 72% SMYS)
2. Tabulated SCF values based upon curve fit of FEA data using a second order polynomial.

Table 5 Stress Concentration Factors (Δσ/ΔP) for Constrained Long Bar Dents

Pipe D/t	Dent Depth (percent d/D)								
	2	4	6	8	10	12	14	16	18
Low Range Pressure Cycle (0 - 50% MOP)									
34	37.9	41.5	46.6	53.2	61.2	70.7	81.7	94.1	108.0
68	78.2	117.5	152.4	182.9	209.0	230.7	248.0	260.9	269.4
High Range Pressure Cycle (50 - 100% MOP)									
34	21.4	27.9	34.5	41.1	47.8	54.6	61.4	68.3	75.2
68	38.8	59.4	78.7	96.7	113.5	129.0	143.2	156.1	167.8
Full Range Pressure Cycle (0 - 100% MOP)									
34	23.6	30.5	37.5	44.4	51.3	58.2	65.1	72.0	78.9
68	70.5	83.7	97.1	110.6	124.3	138.1	152.1	166.2	180.4

Notes:
1. Pressure ranges based upon percentage of MOP, Maximum Operating Pressure (100% MOP corresponds to 72% SMYS)
2. Tabulated SCF values based upon curve fit of FEA data using a second order polynomial.

Table 6 Comparison of Experimental and Analytical Fatigue Results

Sample	Residual Dent Depth (d/D)	Experimental Number of Cycles with ΔP = 50% MOP	Experimental Number of Cycles with ΔP = 100% MOP	Experimental [1] Equivalent Number of Cycles	Analytical [2] Number of Cycles with ΔP = 50% MOP
UD6A-2	1.6%	28,183	79,940	1,307,223	1,494,923
UD12A-3	3.8%	28,183	41,045	684,903	573,940

Notes:
1. The values obtained by determining the equivalent number of cycles assuming an alternating pressure of 50% MOP.
2. These values obtained by calculating fatigue lives assuming upper pressure range of 50% MOP applied.
3. The above dents were installed in 12.75-in x 0.188-in, grade X52 pipe. The dents were installed with no internal pressure in the pipe and were not constrained during cycling.